A MODEL OF STREAMBANK STABILITY INCORPORATING HYDRAULIC EROSION AND THE EFFECTS OF RIPARIAN VEGETATION

Andrew Simon, Research Geologist, USDA-ARS National Sedimentation Laboratory, Oxford, MS, asimon@ars.usda.gov; Natasha Pollen, Research Associate, USDA-ARS National Sedimentation Laboratory, Oxford, MS, npollen@ars.usda.gov

Abstract: Sediment is one of the principle pollutants of surface waters of the United States and sediment eroded from streambank failures has been found to be the single largest contributor to suspended-sediment loads to streams draining unstable systems in the mid-continent. With the recent focus on stream restoration, a quantitative means was needed to predict critical conditions for stability and the effects of riparian vegetation on attaining stable bank geometries. A deterministic bank-stability model was developed in the late 1990's at the USDA-ARS National Sedimentation Laboratory and has undergone substantial enhancements since that time. The original model (Simon et al. 1999) allowed for 5 unique layers, accounted for pore-water pressures on both the saturated and unsaturated parts of the failure plane, and the confining pressure from streamflow. The enhanced Bank Stability and Toe Erosion Model (BSTEM Version 4.1) includes a sub-model to predict bank-toe erosion and undercutting by hydraulic shear. This is based on an excess shear-stress approach that is linked to the geotechnical algorithms. Complex geometries resulting from simulated bank-toe are used as the new input geometry for the geotechnical part of the bank-stability model. The enhanced bank-stability submodel allows the user to select between cantilever and planar failure modes. In addition, the mechanical effects of riparian vegetation are included in Version 4.1, based on the RipRoot model developed by Pollen and Simon (2005). The model has been successfully tested in a diverse range of environments to predict bank failures and to investigate the effects of riparian vegetation on critical conditions for bank stability.

INTRODUCTION

Sediment is one of the principle pollutants of surface waters of the United States and sediment eroded from streambank failures has been found to be the single largest contributor to suspended-sediment loads to streams draining unstable systems in the mid-continent (Simon et al., 2004). With the recent focus on stream restoration, a quantitative means was needed to predict critical conditions for stability and the effects of riparian vegetation on attaining stable bank geometries. Streambank failure can occur by several mechanisms, including cantilever failures of undercut banks, toppling of vertically arranged slabs, rotational slumping, and wedge failures (Thorne et al., 1981). The type of failure reflects the degree of undercutting (if any) by fluvial scour or other mechanisms, and the nature of the bank materials.

In the late 1990's, a deterministic bank-stability model was developed at the USDA-ARS National Sedimentation Laboratory, and has undergone substantial enhancements since that time. The original model (Simon et al., 1999) allowed for 5 unique layers, accounted for pore-water pressures on both the saturated and unsaturated parts of the failure plane, and the confining pressure from streamflow. The enhanced model (Version 4.1) includes a sub-model to predict bank-toe erosion and undercutting by hydraulic shear. This is based on an excess shear-stress approach that is linked to the geotechnical algorithms. Complex geometries resulting from simulated bank-toe are used as the new input geometry for the geotechnical part of the bank-stability model. The enhanced bank-stability sub-model allows the user to select between cantilever and planar failure modes.

The Bank Stability Model combines three limit equilibrium-methods to calculate a Factor of Safety (F_s) for multi-layer streambanks. The methods simulated are horizontal layers (Simon et al., 2000), vertical slices with a tension crack (Morgenstern and Price, 1965) and cantilever failures (Thorne and Tovey, 1981). The model can easily be adapted to incorporate the effects of geotextiles or other bank stabilization measures that affect soil strength. This version of the model assumes hydrostatic conditions below the water table, and a linear interpolation of matric suction above the water table (unless the user's own pore-water pressure data are used).

The Bank Toe Erosion submodel can be used as a tool for making reasonably informed estimates of hydraulic erosion of the bank and bank toe by hydraulic shear stress. The model is primarily intended for use in studies where bank toe erosion threatens bank stability. The effects of erosion protection on the bank and toe can be incorporated to show the effects of erosion control measures. The model estimates boundary shear stress from channel geometry and considers critical shear stress and erodibility of two separate zones with potentially different materials at the

bank and bank toe; the bed elevation is assumed to be fixed. This is because the model assumes that erosion is not transport limited and does not incorporate, in any way, the simulation of sediment transport.

Streambank Stability: The shear strength of saturated soil can be described by the Mohr-Coulomb criterion:

$$\tau_f = c' + (\sigma - \mu_w) \tan \phi' \quad (1)$$

where τ_f = shear stress at failure (kPa), c' =effective cohesion (kPa), σ = normal stress (kPa), μ_w = pore-water pressure (kPa), and ϕ' = effective angle of internal friction (degrees).

In incised stream channels and in arid or semi-arid regions, much of the bank may be above the water table and will usually experience unsaturated conditions. Matric suction (negative pore-water pressure) above the water table has the effect of increasing the apparent cohesion of a soil. Fredlund et al. (1978) defined a functional relationship describing increasing soil strength with increasing matric suction. The rate of increase is defined by the parameter ϕ^b, which is generally between 10º and 20º, with a maximum value of ϕ' under saturated conditions (Fredlund and Rahardjo, 1993). The term ϕ^b varies for all soils, and for a given soil with moisture content (Fredlund and Rahardjo, 1993; Simon et al., 2000). Data on ϕ^b are particularly lacking for alluvial materials. However, once this parameter is known (or assumed) both apparent cohesion (c_a) and effective cohesion (c') can be calculated by measuring matric suction with tensiometers or other devices and by using equation 2. Apparent cohesion incorporates both electro-chemical bonding within the soil matrix and cohesion due to surface tension on the air-water interface of the unsaturated soil:

$$c_a = c' + (\mu_a - \mu_w) \tan \phi^b = c' + \psi \tan \phi^b \quad (2)$$

where c_a = apparent cohesion (kPa), μ_a = pore-air pressure (kPa), and ψ = matric suction (kPa).

Driving forces for streambank instability are controlled by bank height and slope, the unit weight of the soil and the mass of water within it, and the surcharge imposed by any objects on the bank top. The ratio of resisting to driving forces is commonly expressed as the Factor of Safety (F_s), where values greater than one indicate stability and those less than one, instability.

Streambank Stability Algorithms: 1.) Horizontal Layers: The Horizontal Layer method is a further development of the wedge failure type developed by Simon and Curini (1998) and Simon et al. (2000), which in turn is a refinement of the models developed by Osman and Thorne (1988) and Simon et al. (1991). The model is a Limit Equilibrium analysis in which the Mohr-Coulomb failure criterion is used for the saturated portion of the wedge, and the Fredlund et al. (1978) criterion is used for the unsaturated portion. In addition to positive and negative pore-water pressure, the model incorporates layered soils, changes in soil unit weight based on moisture content, and external confining pressure from streamflow. The model divides the bank profile into up to five user definable layers with unique geotechnical properties. The streambank Factor of Safety (F_s) is given by the equation:

$$F_s = \frac{\sum_{i=1}^{I} \left(c_i' L_i + S_i \tan \phi_i^b + \left[W_i \cos \beta - U_i + P_i \cos(\alpha - \beta) \right] \tan \phi_i' \right)}{\sum_{i=1}^{I} \left(W_i \sin \beta - P_i \sin[\alpha - \beta] \right)} \quad (3)$$

where c_i' = effective cohesion of ith layer (kPa), L_i = length of the failure plane incorporated within the ith layer (m), S_i = force produced by matric suction on the unsaturated part of the failure surface (kN/m), W_i = weight of the ith layer (kN), U_i = the hydrostatic-uplift force on the saturated portion of the failure surface (kN/m), P_i = the hydrostatic-confining force due to external water level (kN/m), β = failure-plane angle (degrees from horizontal), α = bank angle (degrees from horizontal), and I = the number of layers.

2.) Vertical Slices: The vertical slice method used only for failures with a tension crack is an adaptation of the method employed in the CONCEPTS model (Langendoen, 2000). As for the Horizontal Layer method, the analysis is a Limit Equilibrium analysis. In addition to the forces incorporated in the Horizontal Layer method, the Vertical Slice method evaluates normal and shear forces active in segments of the failure block. The confining force due to

the water in the channel is modeled by extending the slip surface vertically through the water and applying a horizontal hydrostatic force on the vertical portion of the slip surface. Figure 1 shows an assumed failure block configuration, which is subdivided into slices. The streambank is separated into vertical slices whereby there is an equal number of *J* slices and layers. Each slice is further divided into three subslices to increase the accuracy of the F_s calculations. The calculation of *Fs* is a 4-step iterative process: (1) vertical forces acting on a slice are summed to determine the normal force acting at the base of a slice, $N_{j;}$ (2) horizontal forces acting on a slice are summed to determine the interslice normal force, In *j*; (3) the interslice shear force, $I_{s\,j}$ is computed from $I_{n\,j}$ using the method of Morgenstern and Price (1965); and (4) horizontal forces are summed over all slices to obtain $F_{s.}$ During the first iteration, the interslice normal and shear forces are neglected and the normal force, N_j, equates to:

$$\frac{W_j}{\cos\beta} \tag{4}$$

where W_j is the weight of the j^{th} slice. This first iteration yields the Ordinary F_s. The interslice normal forces are then determined from:

$$I_{n_j} = I_{n_{j-1}} - \left(c_j^{'} L_j + S_j \tan\phi_j^b - U_j \tan\phi_j^{'}\right)\frac{\cos\beta}{F_s} + N_j\left(\sin\beta - \frac{\cos\beta\tan\phi_j^{'}}{F_s}\right) \tag{5}$$

and, in turn, the interslice shear forces are determined from:

$$I_{s_j} = {}^{0.4}\quad I_{n_j}\sin\left(\frac{\pi L_j}{\sum L_j}\right) \tag{6}$$

After the first iteration, for the j^{th} slice out of *J* slices. the normal force, N_j equates to:

$$\frac{W_j + I_{s_{j-1}} - I_{s_j} - \sin\beta\left(\dfrac{c_j^{'} L_j + S_j \tan\phi_j^b - U_j \tan\phi_j^{'}}{F_s}\right)}{\cos\beta + \dfrac{\tan\phi_j^{'}\sin\beta}{F_s}} \tag{7}$$

This completes the second iteration. Often, the calculated interslice normal forces are negative (tension) near the top of the failure block. Since soil is unable to withstand large tensile stresses, a tension crack is assumed to form at the last interslice boundary with tension. Factor of Safety is determined by the balance of forces in horizontal and vertical directions for each subslice and in the horizontal direction for the entire failure block. F_s is given by:

$$F_s = \frac{\cos\beta\sum_{j=1}^{J}\left(c_j^{'} L_j + S_j \tan\phi_j^b + \left[N_j - U_j\right]\tan\phi_j^{'}\right)}{\sin\beta\sum_{j=1}^{J}\left(N_j\right) - P_j} \tag{8}$$

The model then repeatedly iterates through equations 5 to 8 until the value of F_s converges.

3.) Cantilever shear failures: The cantilever shear failure algorithm is a further development of the method employed in the CONCEPTS model (Langendoen, 2000). Put simply, the F_s is the ratio of the shear strength of the soil to the weight of the cantilever. If the bank is submerged then the weight of the layers affected by the water are reduced to their submerged weight. By this method, the vertical hydrostatic confining force is included in the calculation. The F_s is given by:

$$F_s = \frac{\sum_{i=1}^{I}\left(c'_i L_i + S_i \tan\phi_i^b - U_i \tan\phi_i^{'}\right)}{\sum_{i=1}^{I}\left(W_i - P_i\right)} \tag{9}$$

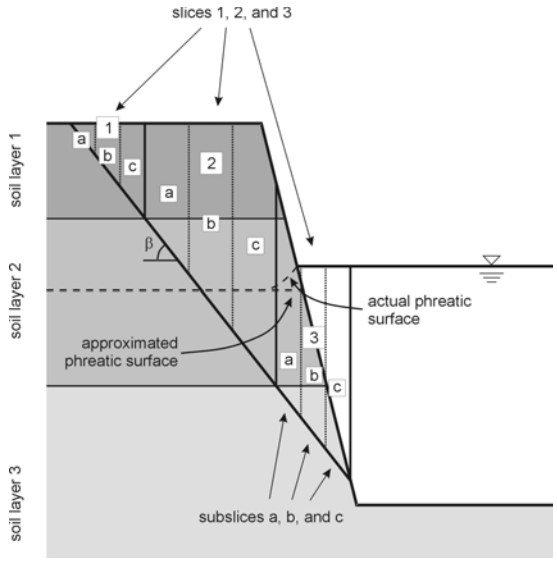

Figure 1 Subdivision of a failure block into slices (Langendoen, 2000).

Vegetation Component: Soil is generally strong in compression, but weak in tension. The fibrous roots of trees and herbaceous species are strong in tension but weak in compression. Root-permeated soil, therefore, makes up a composite material that has enhanced strength (Thorne, 1990). Numerous authors have quantified this enhancement using a mixture of field and laboratory experiments (see Pollen and Simon 2005). Wu et al. (1979) developed a widely used equation that estimates the increase in soil strength (c_r) as a function of root tensile strength, areal density and root distortion during shear:

$$c_r = T_r\,(A_r/A)\,(\cos\theta\tan\phi + \sin\theta) \qquad (10)$$

where c_r = cohesion due to roots (kPa), T_r = tensile strength of roots (kPa), A_r/A = area of shear surface occupied by roots, per unit area (root-area ratio), θ = shear distortion from vertical (degrees), and ϕ = friction angle of soil (degrees). The value of the second bracketed term has been shown to approximate 1.2 under most soil conditions (Wu et al.,1979)..

However, Pollen et al. (2004) and Pollen and Simon (2005) found that perpendicular root models such as those in Equation 10, tend to overestimate root-reinforcement in streambanks, by varying amounts depending on the driving forces acting on the bank, and the number and diameter-distributions of the roots present. To account for this overestimation, Version 4.1 of the model includes an option for the user to reduce the root-reinforcement estimates provided in the BSTEM (taken from Simon and Collison, 2002) by a user-defined percentage (reductions in the range of 20-50% are generally recommended). Future versions of the BSTEM will add a direct link to the RipRoot model developed by Pollen and Simon (2005). The RipRoot model calculates root reinforcement using a progressive breaking algorithm that is driven by the number and species of roots present in the bank, and the driving forces acting on the bank geometry being studied. In previous version of the BSTEM, vegetation was coded to act over the top layer of the streambank regardless of its depth. In Version 4.1, improvements have been made so that the vegetation always acts over the top meter of the bank profile, which fieldwork has shown generally includes the majority of fine roots that contribute to the reinforced root-soil matrix (Simon and Collison, 2002; Pollen et al., 2004).

In addition to stabilizing effects due to root reinforcement, vegetation can affect streambanks by increasing surcharge. Surcharge has both a beneficial and a detrimental effect; it increases the mass acting on a potential failure surface and increases normal stress and, therefore, shear strength due to friction. Whether the net effect is stabilizing or destabilizing depends on the slope of the shear surface and the effective friction angle (ϕ') of the soil, but in most cases it will be destabilizing due to steep shear-surface slopes of streambank failures.

Surcharge due to the mature riparian trees is calculated by multiplying the mass of trees by the stocking density (number of trees per unit area). Tree volume was estimated using the De Vries method (De Vries, 1974):

$$V = \frac{\pi L (d1^2 + d2^2)}{8} \quad (11)$$

where V = volume of wood (m^3), d1 = diameter of trunk at base (m), d2 = diameter of trunk at top (m), and L = length of trunk (m). Volume was converted to mass using an average density of 0.96 g/cm^3 measured for live sycamore, sweetgum and river birch trees in northern Mississippi (Shields et al., 2001). Mass was converted to surcharge by calculating the force per unit area, dividing the tree weight by the root plate area.

Toe Erosion model: Calculation of average boundary shear stress (τ_o): The average boundary shear stress (τ_o) acting on each node of the bank material is calculated using:

$$\tau_o = \gamma_w R S \quad (12)$$

where τ_o = average boundary shear stress (Pa), γ_w = unit weight of water (9.81 kN/m^3), R = local Hydraulic Radius (m) (calculated from the water depth) and S = channel slope (m/m).

The average boundary shear stress exerted by the flow on each node is determined by dividing the flow area at a cross-section into segments that are affected only by the roughness of the bank or bed and then further subdividing to determine the flow area affected by the roughness of each node. The line dividing the bed- and bank- affected segments is assumed to bisect the average bank angle and the average bank toe angle (see Figure 2). The hydraulic radius of the flow on each segment is the area of the segment (A) divided by the wetted perimeter of the segment (P_n). Fluid shear stresses along the dividing lines are neglected when determining the wetted perimeter.

Erodibility and critical shear stress of cohesive materials: A submerged jet-test device has been developed by Hanson (1990) to conduct soil erodibility tests *in situ*. This device has been developed based on knowledge of the hydraulic characteristics of a submerged jet and the characteristics of soil material erodibility. Utilizing this device, Hanson and Simon (2001) developed the following relation between critical shear stress (τ_c) and the erodibility coefficient (k) for cohesive silts, silt-clays and clays:

$$k = 2 \times 10^{-7} \ \tau_c^{-0.5} \quad (13)$$

This relation is very similar to observed trends reported by Arulanandan et al. (1980) in laboratory flume testing of streambed material samples from across the United States. Jet-testing on bank toes suggests that although the exponent is the same, the coefficient is instead 1×10^{-7}.

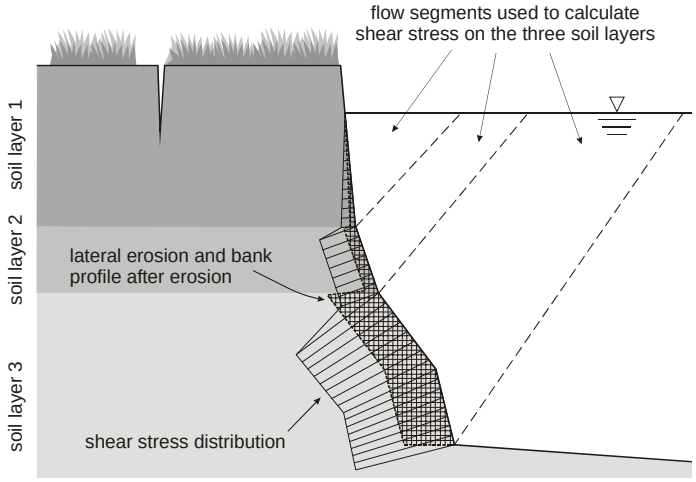

Figure 2 Segmentation of local flow areas and hydraulic radii.

Erosion rates and amounts: An average erosion rate (in m/s) is computed for each node by utilizing an excess-shear stress approach (Partheniades, 1965). This rate is then integrated with respect to time to yield an average erosion distance (in m). This method is similar to that employed in the CONCEPTS model (Langendoen, 2000) except that erosion is assumed to occur normal to the local bank angle, not horizontally:

$$E = k\,\Delta t\,(\tau_0 - \tau_c) \qquad (14)$$

where E = erosion distance (m), k = erodibility coefficient (m^3/N s), Δt = time step (s), τ_0 = average boundary shear stress (Pa), and τ_c = critical shear stress (Pa).

Erodibility and critical shear stress of non-cohesive materials: Resistance of non-cohesive materials is a function of bed roughness and particle size (weight), and is expressed in terms of a dimensionless critical shear stress (Shields 1936):

$$\tau^* = \tau_o / (\rho_s - \rho_w)\, g\, D \qquad (15)$$

where τ^* = critical dimensionless shear stress; ρ_s = sediment density (kg/m^3); ρ_w = water density (kg/m^3); g = gravitational acceleration (m/s^2); and D = characteristic particle diameter (m). Average boundary shear stress (τ_o) is the drag exerted by the flow on the bed and is defined as:

$$\tau_o = \gamma_w\, R\, S_b \qquad (16)$$

where γ_w = unit weight of water (N/m^3); and R = hydraulic radius (area/wetted perimeter)(m). Critical shear stress (τ_c) in dimensional form can be obtained by invoking the Shields criterion and, for hydrodynamically rough beds, utilizing a value of 0.06 for τ^*.

$$\tau_c = 0.06\,(\rho_s - \rho_w)\, g\, D \qquad (17)$$

Thus, the shear stress required to entrain a grain of diameter D can be estimated. Other commonly used values of τ^* are 0.03 and 0.047 (Vanoni and Brookes, 1957).

MODELING EXAMPLE AND SUMMARY

The example analysis provided in Figure 3 shows the BSTEM model run with simulated flow and pore-water pressure data for a site along the Missouri River, Montana (Collison, et al., 2002). In this case, bank-toe erosion (Figure 3a) and bank stability (Figure 3b) were modeled iteratively for a period of 70 days. The effects of decreasing shear strength and Factor of Safety due to loss of matric suction are apparent for the no bank erosion case. Modeling runs were repeated using the bank-toe erosion model. The difference in relative stability is clearly shown by contrasting the two lines plotted in Figure 3b. Simulations without the toe-erosion model would, therefore, have provided overly conservative estimates of bank stability.

The combined bank-stability and toe-erosion models have been used successfully in a variety of locations and alluvial environments in the United States to simulate streambank stability under different flow and pore-water pressure conditions. It has been widely distributed at short courses conducted by the authors at national technical meetings, regional practitioner workshops and for a geomorphology class at the USGS National Training Center. The revised model (Version 4.1) is available on the Web: http://www.ars.usda.gov?Research/docs.htm?docid=5044

Acknowledgement: Eddy Langendoen, USDA-ARS National Sedimentation Laboratory provided critical programming expertise in developing the cantilever failure option and in debugging.

a)

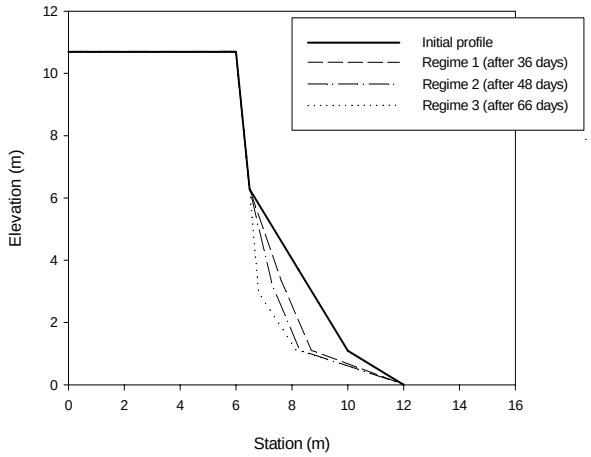

b)

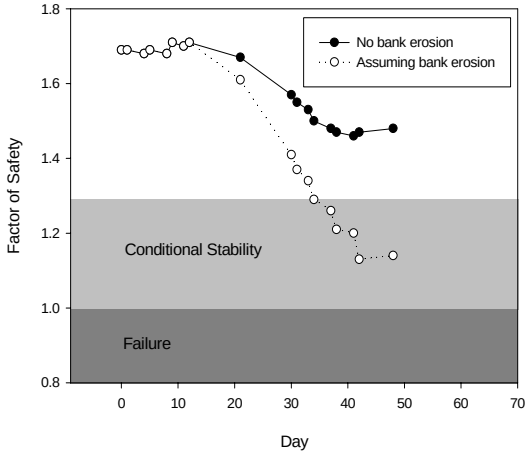

Figure 3 Impact of simulated flow regimes on bank erosion and resulting bank stability at River Mile 1624 (Tveit Johnson site) on the Missouri River, MT.

REFERENCES

Arulanandan K, Gillogley E, Tully R. (1980). "Development of a quantitative method to predict critical shear stress and rate of erosion of natural undisturbed cohesive soils." Technical Report GL-80-5. US Army Engineers Waterways Experiment Station: Vicksburg.

Collison, A.J.C., Layzell, T. and Simon, A. (2002). "Impact of Flow Releases on Bank Stability of the Missouri River, MT", Proceedings of ASCE-EWRI conference, Roanoke, Virginia, May 2002.

De Vries D.G. (1974). "Multi-stage line intersect sampling," Forestry Science 20(2): 129-133

Fredlund D.G, Morgenstern N.R, Widger RA. (1978). "The shear strength of unsaturated soils," Canadian Geotechnical Journal 15: 313-321.

Fredlund D.G, Rahardjo H. (1993). Soil Mechanics of Unsaturated Soils, John Wiley & Sons, Inc., New York.

Hanson G.J. (1990). "Surface erodibility of earthen channels at high stresses. Part II - Development of an in situ testing device," Transactions of the American Society of Agricultural Engineers 33(1): 132-137.

Hanson G.J, Simon A. (2001). "Erodibility of cohesive streambeds in the loess area of the midwestern USA". Hydrological Processes 15: 23-38

Langendoen E.J. (2000). "CONCEPTS - CONservation Channel Evolution and Pollutant Transport System", Research Report 16, US Department of Agriculture Agricultural Research Service National Sedimentation Laboratory, Oxford, MS.

Morgenstern N.R, Price, V.R. (1965). "The analysis of the stability of general slip surfaces." Geotechnique 15: 79-93.

Osman A.M, Thorne C.R. (1988). "Riverbank stability analysis. I: Theory", Journal of Hydraulic Engineering 114(2): 134-150.

Partheniades E. (1965). "Erosion and deposition of cohesive soils", Journal of Hydraulic Engineering 91(1): 105-139.

Pollen, N. and Simon, A. (2005). "Estimating the mechanical effects of riparian vegetation on stream bank stability using a fiber bundle model", Water Resour. Res., 41,No. 7, W0702510.1029/2004WR003801.

Pollen, N., Simon, A., and A. Collison (2004). "Advances in Assessing the Mechanical and Hydrologic Effects of Riparian Vegetation on Streambank Stability". In: S. Bennett and A. Simon, eds. Riparian Vegetation and Fluvial Geomorphology, Water Science and Applications 8, AGU, 125-139.

Shields, A.. (1936). "Anwendung der Aechlichkeitsmechanik und der Turbulenz Forschung auf die Geschiebebewegung", Mitteilungen der Pruessischen Versuchsanstalt fuer Wasserbau and Schiffbau, Berlin.

Shields Jr. F.D, Morin N, Cooper C.M. (2001). "Design of large woody debris structures for channel rehabilitation", Proceedings of the 7th Federal Interagency Sedimentation Conference, Reno, Nevada, 1: II-42 to II-49.

Simon A, Collison A.J.C.(2002). "Quantifying the mechanical and hydrologic effects of riparian vegetation on streambank stability", Earth Surface Processes and Landforms 27(5): 527-546.

Simon, A., Langendoen, E., Bingner, R., Wells, R., Yuan, Y., and Alonso, C. (2004). "Suspended-Sediment Transport and Bed-Material Characteristics of Shades Creek, Alabama and Ecoregion 67: Developing Water-Quality Criteria for Suspended and Bed-Material Sediment", U.S Department of Agriculture-Agricultural Research Service, National Sedimentation Laboratory Technical Report 43.

Simon A, Curini A. (1998). "Pore pressure and bank stability: The influence of matric suction", In Abt S.R, Young-Pezeshk J, Watson C.C (eds.), Water Resources Engineering '98, ASCE: Reston; 358-363.

Simon A, Curini A, Darby S.E, Langendoen E.J. (2000). "Bank and near-bank processes in an incised channel", Geomorphology 35: 183-217.

Simon, A., Curini, A., Darby, S., and Langendoen, E. (1999). "Stream-bank Mechanics and the Role of Bank and Near-Bank Processes in Incised Channels". In*:* Darby, S. and Simon, A., eds. Incised River Channels. John Wiley and Sons, New York. 123-152.

Simon A, Wolfe W.J, Molinas A. (1991). "Mass wasting algorithms in an alluvial channel model", Proceedings of the 5th Federal Interagency Sedimentation Conference, Las Vegas, Nevada, 2: 8-22 to 8-29.

Thorne C.R. (1990). "Effects of vegetation on riverbank erosion and stability", In Thornes JB (ed.), Vegetation and erosion: Processes and Environments, John Wiley & Sons: Chichester; 125-144.

Thorne C.R, Tovey N.K. (1981). Stability of composite river banks. Earth Surface Processes and Landforms 6: 469-484

Thorne C.R., Murphey J.B., Little W.C. (1981). "Bank Stability and Bank Material Properties in the Bluff Line Streams of North-west Mississippi", Appendix D, Report to the Corps of Engineers, Vicksburg District under Section 32 Program, Work Unit 7, USDA-ARS Sedimentation Laboratory, Oxford, Mississippi.

Vanoni, V. A. and Brooks, N. H. (1957). "Laboratory Studies of the Roughness and Suspended Load of Alluvial Streams", Report No. E-68, Sedimentation Laboratory, California Institute of Technology, Pasadena, California.

Wu T.H, McKinnell W.P, Swanston DN. (1979). "Strength of tree roots and landslides on Prince of Wales Island, Alaska", Canadian Geotechnical Journal 16(1): 19-33.